



ORIGINAL ARTICLE

New understanding of aconitine hydrolysis pathway: Isolation, identification and toxicity evaluation based on intermediate products



He Ya-nan^a, Chen Lu-meng^a, Liu Yu^a, Ma Hong-yan^a, Hu Qi^a, Cao Zhi-xing^a, Han Li^a, Xu Run-chun^a, Yang Ming^{b,*}, Tian Yin^{a,*}, Zhang Ding-kun^{a,*}

^a State Key Laboratory of Southwestern Chinese Medicine Resources, Chengdu University of Traditional Chinese Medicine, Chengdu 611137, China

^b State Key Laboratory of Innovation Medicine and High efficiency and Energy Saving Pharmaceutical Equipment, Jiangxi University of Traditional Chinese Medicine, Nanchang 330004, China

Received 1 May 2022; accepted 9 September 2022

Available online 15 September 2022

KEYWORDS

Aconitine;
Hydrolysis law;
Pyroaconitine;
Toxicity evaluation;
Quantum chemical calculation

Abstract Aconitine hydrolysis is deemed to be the guarantee for the safe application of Aconitum phytomedicine. Studies have suggested that hydrolysates of aconitine not only include benzoylaconitine and aconine, but other hydrolysates. Moreover, these hydrolysates maybe have a mutual transformation relationship, which has not been confirmed. Herein, hydrolysates of aconitine and their mutual transformation relationship were studied by the theoretical quantum chemistry, UPLC-Q-TOF-MS, the separation and identification of target products, etc. Then the toxicity of its hydrolysates was evaluated. The results demonstrate that the probability is the same for aconitine hydrolysis to pyroaconitine and benzoylaconitine, but they are difficult to convert to each other. Aconitine hydrolysis has three independent hydrolysis pathways, 1) to indaconitine, 2) to benzoylaconitine, and aconine, 3) to pyroaconitine and to 16-*epi*-pyroaconine. The result of embryotoxicity evaluation on zebrafish was aconitine > indaconitine > benzoylaconitine > α -pyroaconitine > β -pyroaconitine > aconine > 16-*epi*-pyroaconine. In conclusion, aconitine have three independent hydrolysis pathways and the hydrolysates of different pathways cannot be transformed into each other. Pyroaconitine is a hydrolysate of aconitine except for benzoylaconitine, and its tox-

* Corresponding authors at: Jiangxi University of TCM, No. 18 Yunwan Avenue, Nanchang 330004, China (Yang Ming), Chengdu University of TCM, No.1166 Liutai Avenue Chengdu 611137, China (Tian Yin), Chengdu University of TCM, No.1166 Liutai Avenue Chengdu 611137, China (Zhang Ding-kun).

E-mail addresses: heyanan@stu.cdutcm.edu.cn (Y.N. He), 491145843@qq.com (L.M. Cheng), 1071490364@qq.com (Yu. L.), 253557538@qq.com (H.Y. Ma), 953888160@qq.com (Q. Hu), 284886361@qq.com (Z.X. Cao), hanliy@163.com (Li. Han), 309786953@qq.com (R.C. Xu), yangming16@126.com (M. Yang), ytian227@outlook.com (Y. Tian), zhangdingkun@cdutcm.edu.cn (D.K. Zhang).

Peer review under responsibility of King Saud University.



Production and hosting by Elsevier

icity is lower than benzoyleaconitine. More importantly, it clarifies the long-standing debate and provides scientific evidence for the processing and detoxification of Aconitum phytomedicine.

© 2022 The Author(s). Published by Elsevier B.V. on behalf of King Saud University. This is an open access article under the CC BY-NC-ND license (<http://creativecommons.org/licenses/by-nc-nd/4.0/>).

1. Introduction

In East Asia, poisoning events caused by Aconitum phytomedicine are reported every year and diester alkaloids (e.g. aconitine) is the culprit of poisoning (Wendt, et al., 2022; Gao, et al., 2018). Studies have shown that 0.2 mg aconitine can produce a toxic reaction in adults and 1–2 mg can cause death (Ya, et al., 2021). In clinic, Aconitum phytomedicine must take special processing and long-term decoction to hydrolyze the diester alkaloid aconitine to ensure the safety of use (Chan, et al., 2021; Qiu, et al., 2020). Taking aconitine as an example, its classical hydrolysis pathway is the breaking of the ester bond at position C-8, which is hydrolyzed to monoester alkaloid (benzoyleaconitine) with original toxicity of 1/50 ~ 1/500 (Zhang, et al., 2016; Gao, et al., 2022). The benzoyl group at position C-14 is further hydrolyzed to obtain alkanolamine alkaloid (aconine), whose toxicity is only 1/2000 ~ 1/4000 of that of diester aconitine (Zhang, et al., 2016). In recent years, studies have shown that there are many hydrolysis reactions such as deoxidation, dehydration and demethylation in the hydrolysis of aconitine, which has a wide range of hydrolysates (Gao, et al., 2022; Liu, et al., 2022).

Benzoyleaconitine and aconine are recognized hydrolysates of aconitine, but some studies have found that there are other products in recent years. Wang et al. (Wang, et al., 2012) found that benzoyleaconitine and pyroaconitine were the main hydrolysates, after heating and hydrolysis of aconitine. In addition, Zheng et al. (Zheng, et al., 2011) studied the hydrolysis pathway of aconitine and believed that aconitine was hydrolyzed to pyroaconitine first, and then continued to hydrolyze to benzoyleaconitine. Simultaneously, it is considered that

the structure of pyroaconitine is position C-8-C-15 forms an ether ring. In fact, the position C-15 of aconitine is recognized as the carbonyl group. However, it is difficult to add hydroxyl at position C-8 after aconitine C-15 forms carbonyl group, so pyroaconitine may not be the upper hydrolysate of benzoyleaconitine. According to the structure of pyroaconitine, we speculate that there may be two pathways for forming pyroaconitine. One pathway may be the breaking of the ester bond at position C-8 of aconitine and forming enol structure with position C-15. But the enol structure is instability, the ketone structure is formed (Fig. 1A). Another pathway may be dehydration of positions C-8 and C-15 of benzoyleaconitine to form the enol structure and allos-teric to form the ketone structure at position C-15 (Fig. 1B). It is impossible to determine the grade of hydrolysate pyroaconitine due to the lack of standard of pyroaconitine. What's more, most studies remain in the speculative stage, lacking empirical evidence.

Toxicity of aconitine hydrolysate determines the clinical safety of Aconitum phytomedicine. Benzoyleaconitine, which retains the basic structure of aconitine, has much lower toxicity than aconitine. Nevertheless, but it still has cardiotoxicity and neurotoxicity in large doses (Zhang, et al., 2015; Mao, et al., 2021). Aconine also retains the basic structure of aconitine, even though its toxicity is not obvious in the whole animal (Zhang, et al., 2015; Mao, et al., 2021). Multiple hydrolysates are formed after aconitine hydrolysis, but most of their toxicity has not been reported, which restricts our understanding detoxification of aconitine hydrolysis. In this manuscript, we study the hydrolysis process and hydrolysates of aconitine, and compare the toxicity of each hydrolysate, in order to provide more powerful evidence for the hydrolysis law of aconitine.

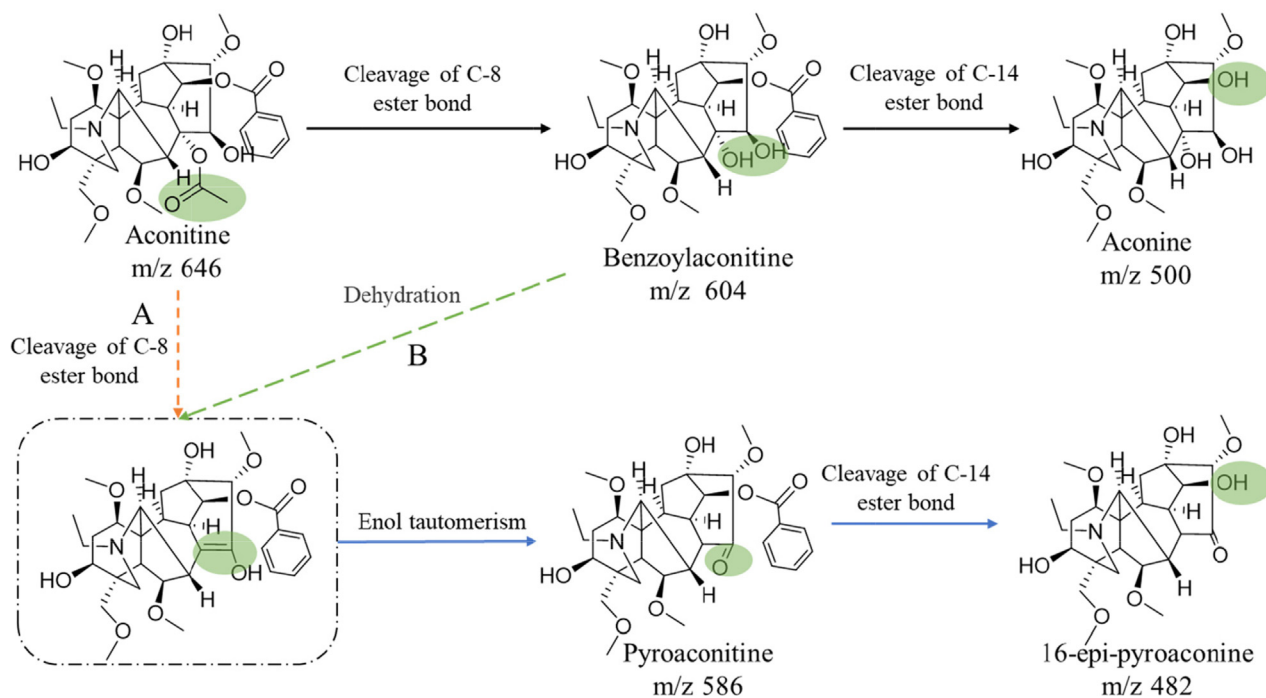


Fig. 1 Possible hydrolysis pathways of aconitine.

2. Materials and methods

2.1. Reagents

Standards of aconine (MUST-16060306), indaconitine (MUST-16101810) were purchased from Chengdu Must Bio-Technology Co., Lt (Chengdu, China). Aconitine (CHB180408) and benzoyleaconine (CHB180309) were purchased from Chroma-Biotechnology Co., Ltd (Chengdu, China). The purity of all compounds is > 98 %. HPLC-grade acetonitrile and methanol were purchased from Fisher Chemical (Pittsburg, USA). Dimethyl sulfoxide and HPLC-grade formic acid were purchased from Chengdu KeLong Chemical Factory (Chengdu, China). Dimethyl sulfoxide-D6 was purchased from Cambridge Isotope Laboratories, Inc (Massachusetts, America).

2.2. Ethics statement

This study was conducted in strict accordance with the recommendations of the Guidelines for the Care and Use of Laboratory Animals of the Ministry of Science and Technology of China. The protocol and experimental designs were approved by the Ethical Committee of Affiliated Hospital of Chengdu University of Traditional Chinese Medicine (Approval ID: 2017BL-003). All possible steps were taken to avoid the animals' suffering at any stage of the experiment.

2.3. Quantum chemical calculation

The electron correlation effects are included by employing density functional theory (DFT)(Hohenberg P and W, 1964) at the M06-2X-D3 level(Zhao and Truhlar, 2008), which include the London-dispersion correction(Grimme, et al., 2010) (Supplementary material 1). The intrinsic reaction coordinate (IRC) (Fukui, 1981) calculations are carried out to verify the transition state (TS) associated with the correct reactant complexes (RC), intermediate (IM) and product complexes (PC) at the same level of theory. The Gibbs free energy of free reactant (Gaconitine) are defined as reference-point. All calculations were carried out with Gaussian 16 program(Frisch, et al., 2016).

2.4. UPLC-Q-TOF-MS analysis

2.4.1. Sample preparation

The standard of 2.09 mg aconitine was prepared in a volumetric flask and dissolved with 100 mL of methanol–water (v/v is 1:99). Accurately measure 10 mL aconitine solution into a glass test tube and weight. Then keep it in 100 °C water bath for 30 min and keep it cold in ice water for 5 min, which is helpful stopping the reaction. Make up for weightlessness and filter through a 0.22 µm micropore film to yield the sample solution for UPLC-Q-TOF-MS analysis.

2.4.2. HPLC condition

The samples are analyzed Thermo Scientific™ Q Exactive™ (ThermoFisher Technologies, Waltham, USA) using a Thermo Scientific Synchronis C18 column (2.1 mm × 100 mm, 1.7 µm). The column temperature is 30 °C and 2 µL of the sam-

ple solution is injected onto the column. The mobile phase is composed of water (A) and acetonitrile (B) using a gradient program of 40 % B for 0–15 min, 40 %–30 % B for 15–19 min, 30 %–30 % B for 19–20 min with a mobile flow rate of 0.2 mL·min⁻¹.

2.4.3. Mass condition

Mass spectrometric scan are obtained by electrospray ionization (H-ESI) in positive and negative ion mode with a scanning interval m/z 50–1500. The main parameters for MS are set as follows: spray voltage (+), 3.5 kV; spray voltage (-), 3.0 kV; capillary temperature, 300 °C; Lens voltage, 50 eV; sheath gas flow rate, 35; aux gas flow rate, 10; sweep gas flow rate, 0.

2.5. Preparation and identification of pyroaconitine and 16-epi-pyroaconitine

2.5.1. Preparation and identification of pyroaconitine

1.5 g aconitine is put into a 100 mL round bottom flask and heat under vacuum at 100 °C for 1 h. DAC dynamic preparation liquid chromatography system is used for separation. Two fractions are obtained and further purified. The solvent in the fraction is recovered under negative pressure. After removing solvation, the residues were dissolved in dichloromethane. Then, filter and recover the solvent to obtain brownish red oil samples. Freeze them in a refrigerator at - 50 °C, white crystals were precipitated, which are compound 1 and compound 2. About 10 mg of these two compounds are dissolved in deuterated dimethyl sulfoxide for nuclear magnetic analysis (AVANCE NEO-700 MHz superconducting fourier Transform nuclear magnetic resonance spectrometry (Bruker, Germany)).

2.5.2. Preparation and identification of 16-epi-pyroaconitine

0.5 g compound 1 is put into a 10 mL round bottom flask with nitrogen and put magnetic stirrer into it with heat at 120 °C and react for 40 min. DAC dynamic preparation liquid chromatography system is used for separation. Then the solvent in the fraction is recovered under negative pressure and obtained white amorphous powder (compound 3). About 10 mg compound 3 is dissolved in deuterated dimethyl sulfoxide for nuclear magnetic analysis.

2.6. HPLC-MS/MS analysis

2.6.1. Samples preparation

The standard of 2.09 mg aconitine, 1.01 mg pyroaconitine, 1.03 mg benzoyleaconitine are respectively prepared in a volumetric flask and dissolved with 100 mL of methanol–water (v/v is 1:99). Accurately measure 10 mL aconitine solution into a glass test tube and weight. Then keep them in 100 °C water bath for 30, 60, 120 min and keep them in ice water for 5 min, which is helpful stopping the reaction. Make up for weightlessness and filter through a 0.22 µm micropore film to yield the sample solution for HPLC-MS/MS.

2.6.2. Preparation of standard solution

The mixed standards containing 1.28 mg aconitine, 1.00 mg aconine, 1.07 benzoyleaconitine, 1.67 mg pyroaconitine, 1.00 mg indaconitine, 1.01 mg 16-epi-pyroaconitine was pre-

pared in a volumetric flask and dissolved with 10 mL of methanol. Working standard solutions were freshly prepared by diluting suitable amounts of the above stock solutions with methanol before injection.

2.6.3. HPLC and mass condition

An Agilent 1260 high performance liquid chromatograph and Agilent 6460C triple-quadrupole tandem mass spectrometry (Agilent Technologies, Santa Clara, USA) is used for the analysis. The fourteen compounds are separated by a Phenomenex Gemini C18 column (4.6 mm × 150 mm, 5 μm) maintained at 30 °C and 0.5 μL of the sample solution is injected into the system. The mobile phase is composed of 0.1 % aqueous formic acid in water (A) and acetonitrile (B) using a gradient program of 2 % B for 0 – 1 min, 20 – 50 % B for 1 – 5 min, 50 – 70 % B for 5 – 10 min, 75 – 100 % B for 10 – 15 min, with a mobile flow rate of 0.45 mL·min⁻¹ (He, et al., 2018).

Mass spectrometric scan are obtained by electrospray ionization (ESI) in positive-ion mode with a scanning interval 100–1000 *m/z*. The main parameters for MS are set as follows: gas temperature, 300 °C; gas flow, 11 L·min⁻¹; nebulizer, 35 psi; capillary voltage, 4000 V; atomizer pressure 15 psi (1 psi = 6.895 Kpa) (He, et al., 2018). MS parameters and MRM transitions of each analyte are shown in Table 1.

2.7. Toxicity evaluation

2.7.1. Zebrafish culture

Zebrafish culture refers to the methods of Westerfield M et al (Westerfield, et al., 1992). Before the experiment, the male and female zebrafish are placed in the spawning tank in the ratio of 1:1, and the male and female zebrafish are separated by a diaphragm. In the early morning of the next day, the diaphragm is removed and the fertilized eggs are obtained. After cleaning and disinfecting the fertilized eggs, transfer them into zebrafish embryo culture water and culture them in a biochemical incubator at (28 ± 2) °C.

2.7.2. Samples preparation

Accurately weigh 1.53 mg aconitine, 1.28 mg indaconitine, 1.64 mg benzoyleaconitine, 1.15 mg aconine, 1.09 mg α-pyroaconitine, 1.81 mg β-pyroaconitine, and 0.96 mg 16-*epi*-pyroaconine. 1 mL dimethyl sulfoxide-water (v/v, 1:1) is added to prepare solutions of aconitine, indaconitine, benzoyleaconitine, aconine, α-pyroaconitine, β-pyroaconitine and 16-*epi*-pyroaconine. And put them in 4 °C refrigerator for standby. Dilute with chemical fish water to different concentrations before use. Furthermore, the concentration of dimethyl sulfoxide is less than 0.5 %.

2.7.3. Acute toxicity evaluation

Zebrafish embryos (1 dpf, 10 per pore) are randomly selected in 24 pore plates, and set 3 multiple pores. The minimum total lethal concentration (LC₁₀₀) and maximum non-lethal concentration (LC₀) of aconitine, indaconitine, benzoyleaconitine, aconine, α-pyroaconitine, β-pyroaconitine and 16-*epi*-pyroaconine are determined by pre-experiment. According to their LC₁₀₀ and LC₀, six gradient concentrations are set for each compound. 1 mL of corresponding concentration of compound is added to each pore and the control group is added with chemical fish water. Then cultured in a biochemical incubator at (28 ± 2) °C for 72 h. Count and remove the dead zebrafish every 24 h, and record the death number and toxicity of zebrafish in each group. The median lethal dose (LC₅₀) and 10 % lethal concentration (LC₁₀) were calculated by SPSS 21.0.

2.7.4. Embryotoxicity evaluation

According to the results of acute toxicity, the 7 compounds are set in minimum (1/9 LC₀), low (1/3 LC₀), medium (LC₀) and high (LC₁₀) dose concentration groups respectively. Zebrafish embryos (4 hpf, 10 per pore) are randomly selected in 24 pore plates and set 3 multiple pores. 1 mL of corresponding concentration of the compound is added to each pore, and chemical fish water is added to the control group. After continuous administration in a biochemical incubator at (28 ± 2) °C for 48 h, the effects of 7 compounds on embryonic development of zebrafish are observed and the development of heart, liver and intestine of zebrafish are recorded.

3. Results

3.1. Result of quantum chemical calculation

The quantum chemical calculation of hydrolysis reaction pathways is carried out according to the previous speculative results (Supplementary material). As shown in Fig. 2, the theoretical results reveal that the activation energy barrier for the ester hydrolyzation to produce the benzoyleaconitine of vicinal diol structure (intermediate IM1 or IM2), which corresponds to the destruction of aconitine C-8 ester bond and transition state TS1 (37.4 kcal/mol), is close to that (TS4, 37.8 kcal/mol) for the elimination reaction of forming enol structure at C-8 and C-15 (intermediate IM5 or IM6). It indicates that the probabilities of forming enol and vicinal diol structures are almost the same as each other. However, the activation energy barrier (TS2) for the elimination reaction of the benzoyleaconitine of vicinal diol structure (IM2) to form enol structure (IM3) is 55.8 kcal/mol and much higher than that for the ester

Table 1 The detected ion pairs of fourteen alkaloids.

Name	Molecular ion (<i>m/z</i>)	Fragment ion (<i>m/z</i>)	Fragmentor (V)	Collision energy (ev)
Aconitine	646.3	105.1	180	50
Indaconitine	630.3	105.1	200	46
Benzoyleaconitine	604.3	105.0	180	45
Pyroaconitine	586.1	104.9	185	50
Aconine	500.3	58.1	180	48
16- <i>epi</i> -pyroaconine	482.2	58.1	180	45

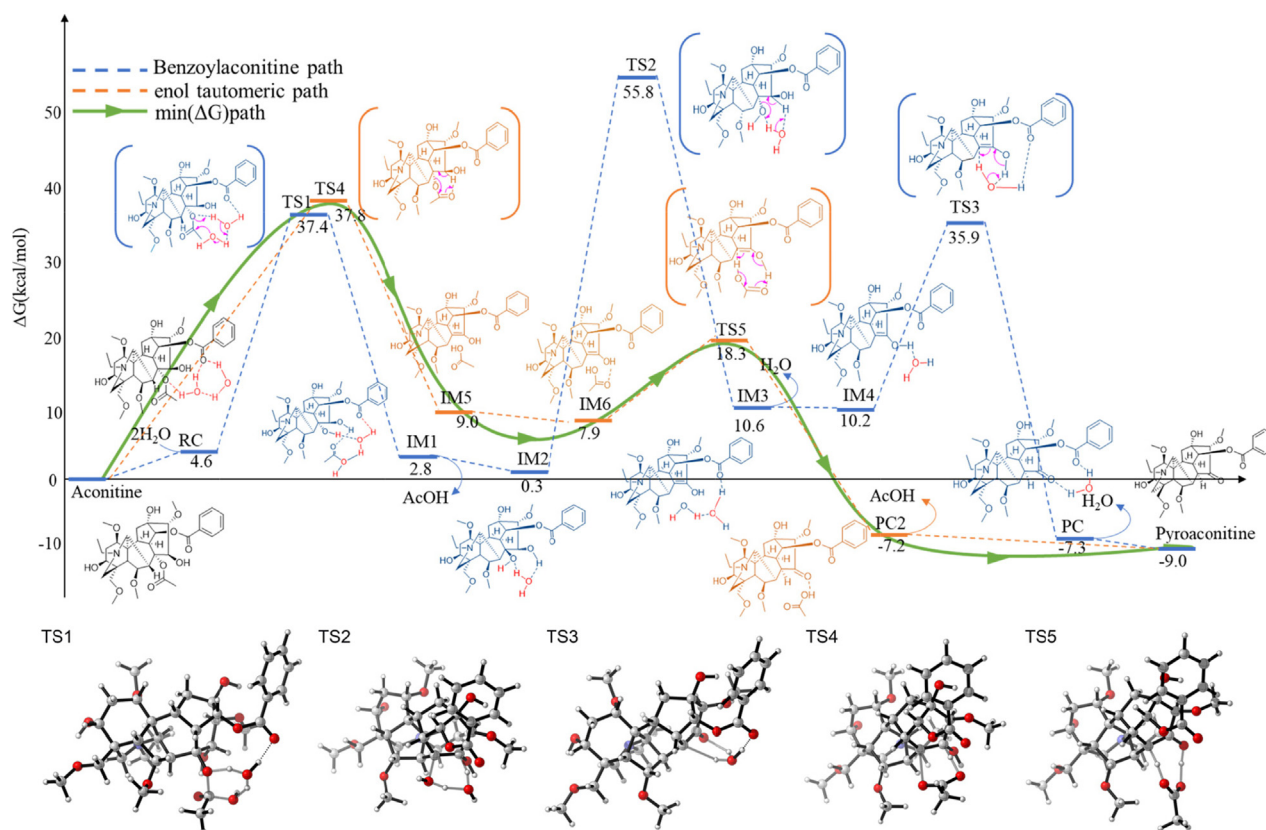


Fig. 2 DFT-computed relative energy profiles (in kcal/mol) for the hydrolysis reaction of aconitine along two pathways at the M06-2X-D3/6-31G(d,p)/SMD(Water) level.

hydrolyzation (TS1), which suggest that the vicinal diol and enol in aconitine structure are difficult to transform into each other. Moreover, the relative free energy of transition state TS5 is 18.3 kcal/mol and much lower than the other transition states, which indicate that the keto-enol tautomerization to form pyroaconitine are favorable in this reaction system. In brief, pyroaconitine and benzoylaconitine cannot be converted to each other, and the C-15 of pyroaconitine is a carbonyl rather than ether ring.

3.2. Results of UPLC-Q-TOF-MS

Six compounds are extracted from aconitine hydrolysate according to high-resolution mass spectrometry data, retention time and multistage fragment ions (Table 2 and Fig. 3). Compared with the literature and standard, m/z of 646.32 is aconitine whose MS^n fragmentation ions is shown in Fig. 3A. m/z of 630.33 is inaconitine, which is the dehydroxylation product of aconitine at position C-15 (Fig. 3B). m/z of 604.31 is identified as benzoylaconitine, which is an ester bond breaking product of aconitine at position C-8 (Fig. 3C). m/z 500.29 is identified as aconine, which is an ester bond breaking of benzoylaconitine at position C-14 (Fig. 3E). Due to lack standards of m/z 586.30 and 482.28, their compound information is speculated by the functions of mass calculators and formula finder of peakview software. The results show that m/z 586.30 is pyroaconitine and m/z 482.28 is 16-*epi*-pyroaconitine (Fig. 3D and 3F). It can be preliminarily judged from the above results

that the hydrolysates of aconitine are basically consistent with those reported in the literature, but it needs a more in-depth analysis on whether there is a relationship between these products.

3.3. Identification of pyroaconitine and 16-*epi*-pyroaconitine

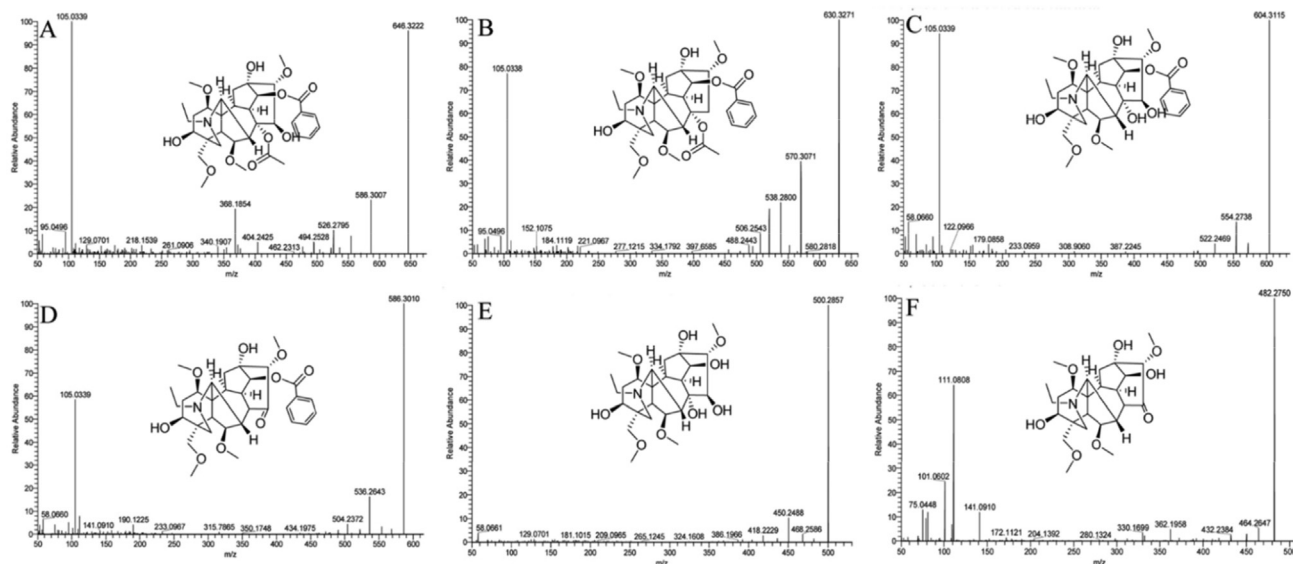
The structure of compounds was determined by ^1H NMR and ^{13}C NMR analysis and comparison with the data in the published literature. m/z 586.30 is identified as pyroaconitine, and it has two configurations, α and β (Fig. 4A and 4B, Supplementary material 2). m/z 482.28 is identified as 16-*epi*-pyroaconitine (Fig. 4C, Supplementary material 2). In fact, 16-*epi*-pyroaconitine also has isomerism of R and S at position C-16. Unfortunately, the other configuration has not been separated.

3.4. Results of HPLC-MS/MS

The hydrolysis products of aconitine at different times are quantitatively analyzed by HPLC-MS/MS. The results show that the hydrolysates of aconitine are inaconitine, benzoylaconitine, pyroaconitine, aconine and 16-*epi*-pyroaconitine in 30–60 min, which is consistent with the results of UPLC-Q-TOF-MS (Table 2). The results also showed that the content of hydrolysate was related to heating time. For instance, the contents of inaconitine and pyroaconitine decreased gradually, while the contents of benzoylaconitine, aconine and 16-

Table 2 Mass spectrum identification results of aconitine hydrolysate.

RT (min)	Compound	Ion mode	Formula	Theoretical mass (m/z)	Experimental mass (m/z)	Error (ppm)	MS ⁿ fragmentation ions (m/z)
3.76	Aconitine	[M + H] ⁺	C34H47NO11	646.32	646.32	0.77	586.30, 368.19, 105.03
3.59	Indaconitine	[M + H] ⁺	C34H46NO10	630.33	630.33	0.16	570.31, 538.28, 105.03
2.33	benzoylaconitine	[M + H] ⁺	C32H45NO10	604.31	604.31	0.83	554.28, 522.25, 105.03, 58.07
3.07	pyroaconitine	[M + H] ⁺	C32H43NO9	586.30	586.30	1.02	568.30, 536.26, 105.03
1.78	Aconine	[M + H] ⁺	C25H41NO9	500.29	500.29	0.00	468.26, 450.25, 58.07
1.73	16- <i>epi</i> -pyroaconine	[M + H] ⁺	C25H39NO8	482.27	482.28	0.62	464.26, 111.08, 75.04

**Fig. 3** Mass spectroscopic fragmentation (A, Aconitine; B, Indaconitine; C, Benzoylaconitine; D, pyroaconitine; E, Aconine; F, 16-*epi*-pyroaconine).**Table 3** Hydrolysate content of aconitine at different time (n = 6).

Content (μg)	0 min	30 min	60 min	120 min
Aconitine	209.00	1.12 \pm 0.41	0.48 \pm 0.15	0.37 \pm 0.02
Indaconitine	ND	0.48 \pm 0.34	0.01 \pm 0.02	ND
Benzoylaconitine	ND	74.20 \pm 2.42	112.32 \pm 5.91	154.94 \pm 1.34
Pyroaconitine	ND	47.55 \pm 0.72	35.02 \pm 1.90	20.73 \pm 0.19
Aconine	ND	2.97 \pm 0.42	6.93 \pm 0.17	17.00 \pm 1.46
16- <i>epi</i> -pyroaconine	ND	0.09 \pm 0.08	0.25 \pm 0.06	0.30 \pm 0.23

Note: ND, not detected.

epi-pyroaconine increased gradually (Table 3). In addition, we also explored the hydrolysates of benzoylaconitine and pyroaconitine (Table 4). The results suggested that the hydrolysate of benzoylaconitine is only aconitine, and the hydrolysate of pyroaconitine is only 16-*epi*-pyroaconine. This result further illustrates that there is no mutual conversion between pyroaconitine and benzoylaconitine, and there are three hydrolysis pathways of aconitine.

3.5. Toxicity evaluation

3.5.1. Acute toxicity

The pre-experimental results showed that the LC₁₀₀ of 7 compounds were 5.13 mg·L⁻¹ aconitine, 3.41 mg·L⁻¹ indaconitine,

61.50 mg·L⁻¹ benzoylaconitine, 123.00 mg·L⁻¹ α -pyroaconitine, 100.00 mg·L⁻¹ β -pyroaconitine, 71.88 mg·L⁻¹ aconine and 96.80 mg·L⁻¹ 16-*epi*-pyroaconine. The LC₀ of 7 compounds were 1.68 mg·L⁻¹ aconitine, 0.89 mg·L⁻¹ indaconitine, 20.13 mg·L⁻¹ benzoylaconitine, 26.24 mg·L⁻¹ α -pyroaconitine, 37.17 mg·L⁻¹ β -pyroaconitine, 29.80 mg·L⁻¹ aconine and 31.62 mg·L⁻¹ 16-*epi*-pyroaconine. The results of acute toxicity test were shown that the LC₅₀ and LC₁₀ of indaconitine is minimum, which means it has strongest toxicity, followed aconitine, benzoylaconitine, 16-*epi*-pyroaconine, aconine, β -pyroaconitine and α -pyroaconitine. Notably, the LC₅₀ and LC₁₀ of 16-*epi*-pyroaconine, aconine, β -pyroaconitine and α -pyroaconitine are close, especially LC₁₀, which means their toxicity is similar (Table 5).

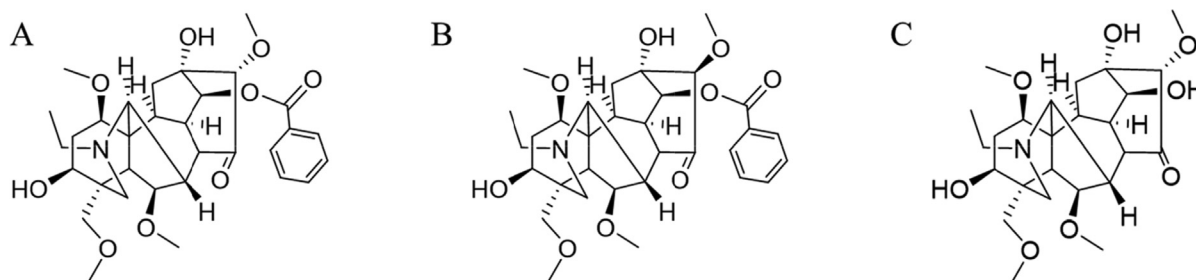
Table 4 Hydrolysate Content of benzoyleaconitine and pyroaconitine at different time(n = 6).

Content (μg)	Benzoyleaconitine	Pyroaconitine	Aconine	16- <i>epi</i> -pyroaconine
0 min	58.50	ND	ND	ND
30 min	45.98 \pm 1.11	ND	0.37 \pm 0.02	ND
60 min	46.52 \pm 1.09	ND	0.42 \pm 0.06	ND
120 min	45.30 \pm 1.46	ND	1.24 \pm 0.03	ND
0 min	ND	87.50	ND	ND
30 min	ND	78.30 \pm 4.30	ND	2.74 \pm 0.22
60 min	ND	78.69 \pm 1.56	ND	3.69 \pm 0.15
120 min	ND	66.79 \pm 7.12	ND	12.50 \pm 2.79

Note: ND, not detected.

Table 5 The results of acute toxicity in 7 compounds.

compounds	LC ₅₀ (mg·L ⁻¹)	95 % confidence interval	LC ₁₀ (mg·L ⁻¹)	95 % confidence interval
aconitine	2.80	2.60–3.00	1.91	1.65–2.11
indaconitine	1.80	1.64–1.98	1.12	0.95–1.25
benzoyleaconitine	37.20	34.80–39.78	26.36	23.07–28.82
α -pyroaconitine	64.52	59.69–70.25	42.27	36.20–46.87
β -pyroaconitine	59.90	50.83–69.11	40.52	26.85–48.14
aconine	50.59	43.84–57.09	37.10	26.20–43.04
16- <i>epi</i> -pyroaconine	48.74	40.90–56.67	32.78	20.82–39.48

**Fig. 4** The structure of α -pyroaconitine (A), β -pyroaconitine (B) and 16-*epi*-pyroaconine (C).

3.5.2. Embryotoxicity

The results showed that aconitine and its hydrolysates showed strong embryotoxicity at concentration of LC₁₀ and LC₀ compared with the blank control group, which could cause obvious deformity and melanin reduction of 24 hpf embryos, as well as delayed hatching of some embryos (Fig. 5). Furthermore, the main teratogenic manifestations of 48 hpf embryos were pericardial edema, yolk sac edema, trunk bending and slow heart-beat, indicating that aconitine and its hydrolysates had early embryonic development toxicity at concentration of LC₁₀ and LC₀. It is worth noting that aconitine at 0.19 mg·L⁻¹, indaconitine at 0.30 mg·L⁻¹, benzoyleaconitine at 2.24 mg·L⁻¹ and α -pyroaconitine at 10.93 mg·L⁻¹ at still showed embryonic malformation at a lower concentration (malformation rate > 50 %). β -pyroaconitine at 27.92 mg·L⁻¹, aconine at 29.90 mg·L⁻¹ and 16-*epi*-pyroaconine at 31.62 mg·L⁻¹ have little embryonic toxicity (malformation rate less than 10 %).

4. Discussion

In the past few decades, the generally accepted detoxification principle of aconitine is that diester alkaloids are hydrolyzed to benzoyleaconitine and then hydrolyzed to aconine (Fig. 6A). Pyroaconitine has always been considered as the intermediate product from aconitine to benzoyleaconitine for two reasons. One is its content increased first and then decreased in the hydrolysis process, while the content of benzoyleaconitine increased all the time (Zheng, et al., 2011). Another reason is that the structure of pyroaconitine is not clear. Some literatures believe that the C-8 and C-15 positions of pyroaconitine are an oxirane (Zheng, et al., 2011), and some studies believe that C-15 position is a carbonyl group (Tan, et al., 2011). The two structures are isomeric and cannot be distinguished by mass spectrometry. In this study, the C-15 position of pyroaconitine was determined as carbonyl group by

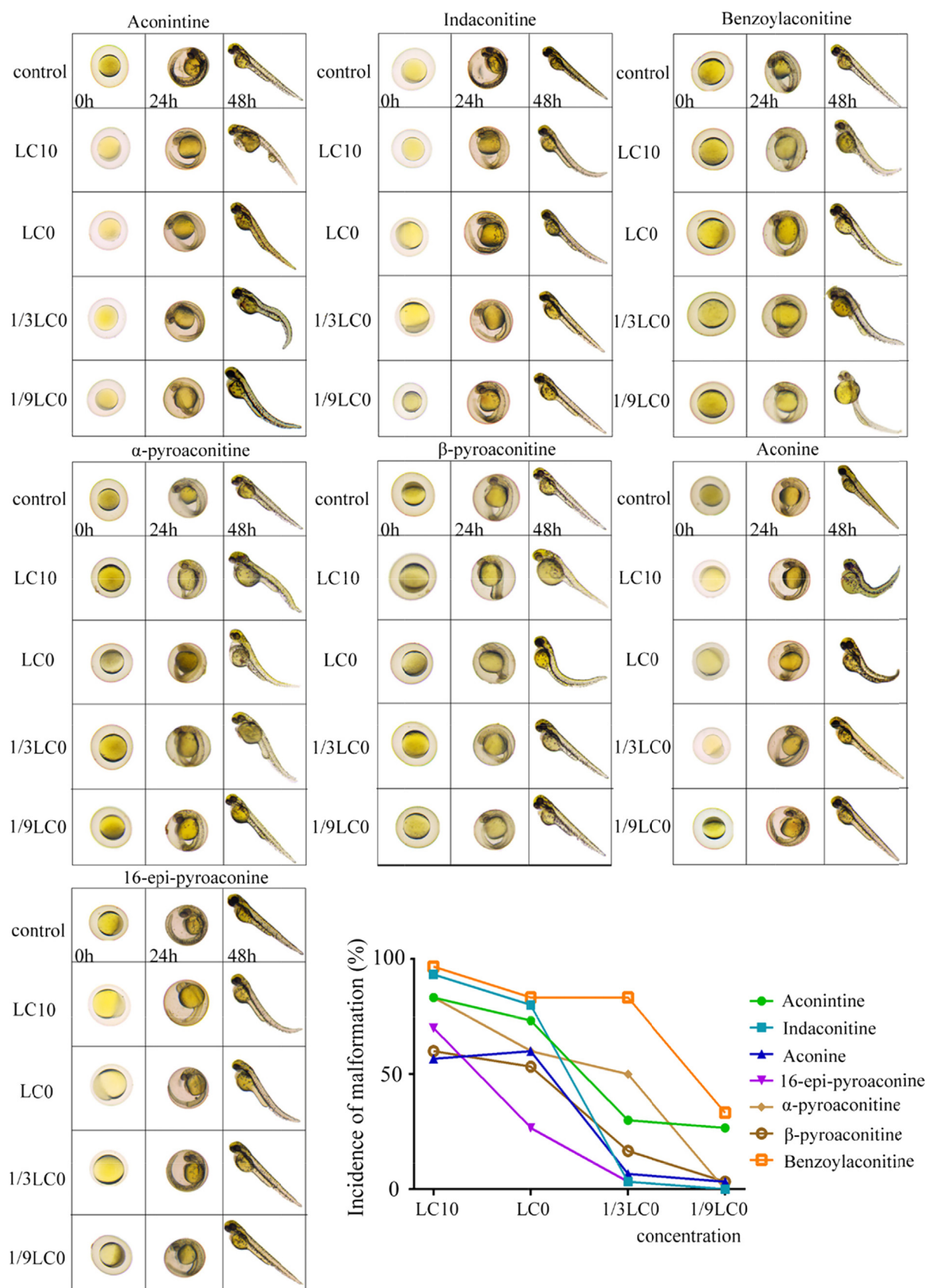


Fig. 5 Embryotoxicity of aconitine, indaconitine, benzoylaconitine, α -pyroaconitine, β -pyroaconitine, aconine and 16-*epi*-pyroaconitine at different concentration.

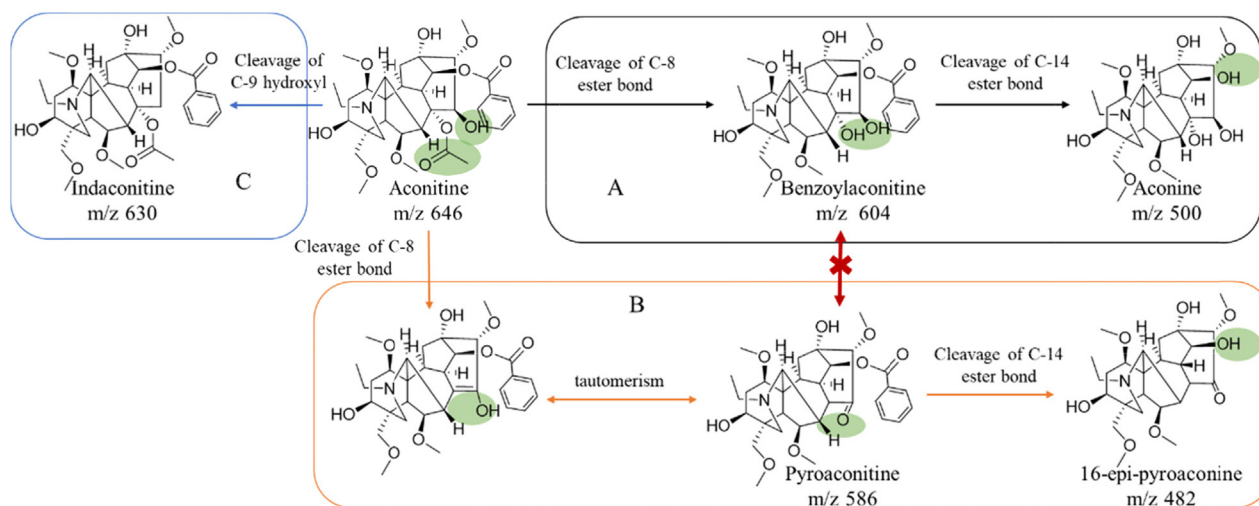


Fig. 6 Three hydrolysis pathways of aconitine (A, aconitine hydrolyze to benzoylaconitine, and aconine; B, aconitine hydrolyze to pyroaconitine and to 16-*epi*-pyroaconitine; C, aconitine hydrolyze to indaconitine).

nuclear magnetic analysis. Meanwhile, pyroaconitine was also proved to be converted to 16-*epi*-pyroaconitine rather than benzoylaconitine (Fig. 6B). A recent study has speculated that the intermediate product of the hydrolysis of hypaconitine (one of diester aconitines) to benzoylhypaconitine is 8,15-oxirane-benzoylhypaconine (m/z is 556), whose is an isomer of pyrohypaconitine (Qiu, et al., 2021). However, there are no similar products found in the separated hydrolysates in this study, which may be caused by the instability of the product or its low content. Therefore, we speculate that the decrease of pyroaconitine content may be hydrolyzed to 16-*epi*-pyroaconitine or other next-order hydrolysates.

Aconitine is an important toxic component in *Aconitum* phytomedicine. It was found that the toxicity of aconitine was mainly related to the substituents at positions C-4, C-8 and C-14. Angélica M. et al. (Angélica M. and Alejandro A., 2004) compared the toxicity of C-14 and C-4 substituents as arylacyl or arylester, respectively. They found that the toxicity of C-14 is significantly stronger than C-4. Hong et al. (Hong and Qiu, 2008) found that the active center of aconitine is the positive region. The more charge the positive region carries, the stronger its binding with biological receptors, thus its toxicity is stronger. Aconitine has strong electron absorbing groups at positions C-8 and C-14, so it has the strongest toxicity. After aconitine hydrolysis, the ester bond at C-8 position was broken and the charge in the positive region decreased. This means that its binding with biological receptors is weakened, so the toxicity of benzoylaconitine and pyroaconitine is lower than that of aconitine. Hong et al. (Hong and Qiu, 2008) also found that the benzoyl group at the C-14 position of aconitine was an important factor affecting toxicity. When the ester group at position C-14 is hydrolyzed to hydroxyl, it will affect the charge distribution and frontier orbit of the molecule to weak its interaction with the receptor. This also explains why aconine is less toxic than benzoylaconitine. In addition, the toxicity of α -pyroaconitine and β -pyroaconitine is also significantly different, which may be related to the spatial isomerization of C-16 substituent. The stereoconfiguration of compounds can also determine their binding force to biological receptors. The stereoisomerism of C-16 position of β -pyroaconitine may weaken the molecular force with biological

receptor to reduce the toxicity. In recent years, some researchers began to pay attention to the relationship between toxicity and structure of *Aconitum* alkaloids. However, the research on the relationship between structure and toxicity of *Aconitum* alkaloids is not perfect, and some laws between toxicity and structure need to be further studied.

Because of its toxicity, the processing of plant medicine containing aconitine has attracted much attention. Hydrolysis is the most likely detoxification reaction during the processing. Therefore, knowing more about the hydrolysates of aconitine will help to prevent the under or over processing of plant medicine containing aconitine and improve their safety and activity. In this study, this study explained the hydrolysis pathway of aconitine from the perspective of monomers, and found that the pyroaconitine pathway was the least toxic. However, the hydrolysates of aconitine are still mainly benzoylaconitine in the complex processing process, while pyroaconitine is rarely reported, which may be caused by the low content. It is necessary to further study the factors affecting the hydrolysis direction of aconitine in complex processing systems, and effectively control the hydrolysis direction so that it can be transformed into a less toxic way. This is of great value for improving the safety of plant medicine containing aconitine and promoting the innovation of traditional technology.

5. Conclusions

This combined experimental and quantum-chemical study demonstrated that there were three independent hydrolysis pathways of aconitine hydrolysis, and pyroaconitine and benzoylaconitine could not be transformed into each other. The toxicity of hydrolysates from three hydrolysis pathways of aconitine was compared for the first time, which develop a deeper understanding for the hydrolysis process of aconitine, and provide a novel approach for the study of natural medicine.

Declaration of Competing Interest

The authors declare that they have no known competing financial interests or personal relationships that could have appeared to influence the work reported in this paper.

Acknowledgments

This study was supported by National Key Research and Development Program (2018YFC1707205, China), Open Project of State key Laboratory of Innovation Medicine and High Efficiency and Energy Saving Pharmaceutical Equipment in Jiangxi University of Traditional Chinese Medicine (GZSYS202003, China), Special Project for Scientific and Technological research of Sichuan Provincial Administration of Traditional Chinese Medicine (2021MS016, China), Sichuan Provincial Science and Technology Innovation (Seeding Project) Cultivation Project (2021041, China). The author would like to thank Xie Long, Zhou Jin and Wang Di (State Key Laboratory of Southwestern Chinese Medicine Resources, Chengdu University of Traditional Chinese Medicine, Chengdu, China). As well as thank Pan Yuan and Li Hong-xiang (Innovative Institute of Chinese Medicine and Pharmacy, Chengdu University of Traditional Chinese Medicine, Chengdu, China).

Author contributions

He Ya-nan, Yang Ming, Zhang Ding-kun designed this study, Chen Lu-meng, Liu Yu, Hu Qi, Cao Zhi-xing and Tian Yin performed experiments, Han Li, Xu Run-chun supplied materials and analytic tools, He Ya-nan, Ma Hong-yan, Zhang Ding-kun and Tian Yin analyzed data. He Ya-nan, Zhang Ding-kun and Tian Yin wrote the paper. Yang Ming, Zhang Ding-kun and He Ya-nan provided financial assistance.

Appendix A. Supplementary material

Supplementary data to this article can be found online at <https://doi.org/10.1016/j.arabjc.2022.104255>.

References

- Angélica, M.B.R., Alejandro, A.N.O., 2004. A QSAR analysis of toxicity of Aconitum alkaloids. *Fundam. Clin. Pharmacol.* 18, 699–704. <https://doi.org/10.1111/j.1472-8206.2004.00280.x>.
- Chan, Y.T., Wang, N., Feng, Y., 2021. The toxicology and detoxification of Aconitum: traditional and modern views. *Chin. Med.* 16, 61. <https://doi.org/10.1186/s13020-021-00472-9>.
- Frisch MJ and Trucks GW and Schlegel HB, *et al.* Gaussian 16. ed.: Gaussian, Inc. Wallingford, CT 2016.
- Fukui Kenichi. 1981. The path of chemical reactions - the IRC approach. *Acc Chem Res.* 14, 363-368. <https://doi.org/10.1021/ar00072a001>.
- Gao, Y., Fan, H., Nie, A., *et al.*, 2022. Aconitine: a review of its pharmacokinetics, pharmacology, toxicology and detoxification. *J. Ethnopharmacol.* 293,. <https://doi.org/10.1016/j.jep.2022.115270>.
- Gao, X., Hu, J., Zhang, X., *et al.*, 2018. Research progress of aconitine toxicity and forensic analysis of aconitine poisoning. *Forensic Sci. Res.* 5, 25–31. <https://doi.org/10.1080/20961790.2018.1452346>.
- Grimme, S., Antony, J., Ehrlich, S., *et al.*, 2010. A consistent and accurate ab initio parametrization of density functional dispersion correction (DFT-D) for the 94 elements H-Pu. *J. Chem. Phys.* 132,. <https://doi.org/10.1063/1.3382344> 154104.
- He, Y.N., Ou, S.P., Xiong, X., *et al.*, 2018. Stems and leaves of *Aconitum carmichaelii* Debx. as potential herbal resources for treating rheumatoid arthritis: Chemical analysis, toxicity and activity evaluation. *Chin. J. Nat. Med.* 16, 644–652. [https://doi.org/10.1016/s1875-5364\(18\)30104-3](https://doi.org/10.1016/s1875-5364(18)30104-3).
- Hohenberg, P., Kohn, W., 1964. Inhomogeneous electron gas. *Phys. Rev. B* 136, B864–B871.
- Hong, B., Qiu, Y.Q., 2008. Density functional theory study on the mechanism of hydrolysis and detoxification of diester aconitine in *Aconiti Lateralis Praeparata*. *J. Mol. Sci.*, 216–219
- Liu, Y., Yang, X., Zhou, C., *et al.*, 2022. Unveiling dynamic changes of chemical constituents in raw and processed Fuzi with different steaming time points using desorption electrospray ionization mass spectrometry imaging combined with metabolomics. *Front. Pharmacol.* 13,. <https://doi.org/10.3389/fphar.2022.842890> 842890.
- Mao, L., Jin, B., Chen, L., *et al.*, 2021. Functional identification of the terpene synthase family involved in diterpenoid alkaloids biosynthesis in *Aconitum carmichaelii*. *Acta Pharm. Sin. B* 11, 3310–3321. <https://doi.org/10.1016/j.apsb.2021.04.008>.
- Qiu, Z.D., Chen, J.L., Zeng, W., *et al.*, 2020. Real-time toxicity prediction of *Aconitum* stewing system using extractive electrospray ionization mass spectrometry. *Acta Pharm. Sin. B* 10, 903–912. <https://doi.org/10.1016/j.apsb.2019.08.012>.
- Qiu, Z.D., Zhang, X., Wei, X.Y., *et al.*, 2021. Online discovery of the molecular mechanism for directionally detoxification of Fuzi using real-time extractive electrospray ionization mass spectrometry. *J. Ethnopharmacol.* 277,. <https://doi.org/10.1016/j.jep.2021.114216> 114216.
- Tan, P., Liu, Y., Guan, J., *et al.*, 2011. Studies on new hydrolysate of aconitine using HPLC-MS(n) and quantum chemistry calculation. *Chin. J. Chin. Mater. Med.* 36, 2099–2101.
- Wang, F.F., Song, Z.H., Zhang, L.L., *et al.*, 2012. Identification of hydrolysates and alcoholysates of aconitum alkaloids. *Chin. J. Chin. Mater. Med.* 37, 1564–1569.
- Wendt, S., Lübbert, C., Begemann, K., *et al.*, 2022. Poisoning by plants. *Dtsch. Arztebl. Int.* <https://doi.org/10.3238/arztebl.m2022.0124>.
- Westerfield, M., Wegner, J., Jegalian, B.G., *et al.*, 1992. Specific activation of mammalian Hox promoters in mosaic transgenic zebrafish. *Genes Dev.* 6, 591–598. <https://doi.org/10.1101/gad.6.4.591>.
- Ya, Y., Zhixiang, Z., Chao, L., *et al.*, 2021. Reflections on the aconitine poisoning. *J. Forensic Sci.* 66, 2035–2040. <https://doi.org/10.1111/1556-4029.14766>.
- Zhang D.K. and Li R.S. and Han X., *et al.* 2016. Toxic Constituents Index: A Toxicity-Calibrated Quantitative Evaluation Approach for the Precise Toxicity Prediction of the Hypertoxic Phytomedicine—Aconite. *Front Pharmacol.* 7, 164. <https://doi.org/10.3389/fphar.2016.00164>. eCollection 2016.
- Zhang, D.K., Wang, J.B., Yang, M., *et al.*, 2015. Exploring in integrated quality evaluation of Chinese herbal medicines: the integrated quality index (IQI) for aconite. *Chin. J. Chin. Mater. Med.* 40, 2582–2588.
- Zhao Yan and Truhlar Donald G. 2008. The M06 suite of density functionals for main group thermochemistry, thermochemical kinetics, noncovalent interactions, excited states, and transition elements: two new functionals and systematic testing of four M06-class functionals and 12 other functionals. *Theor Chem Acc.* 120, 215–241. <https://doi.org/10.1007/s00214-007-0310-x>.
- Zheng, Q., Lu, H.W., Hao, W.W., *et al.*, 2011. Study on hydrolysis of *Aconitum* Alkaloids and quantitative analysis method of their hydrolysates. *Chin. Pharm.* 46, 652–656.